

Original Research

Study on Remote Sensing Image Classification of Oasis Area Based on ENVI Deep Learning

Hong Ma¹, Wenju Zhao^{1*}, Fenhua Li², Honghua Yan², Yuhang Liu¹

¹College of Energy and Power Engineering, Lanzhou University of Technology, Lanzhou 730050, China

²Taolai River Basin Water Resources Utilization Center, Gansu Provincial Department of Water Resources, Jiuquan 735000, China

Received: 14 December 2022

Accepted: 2 February 2023

Abstract

In this paper, based on the Landsat multispectral remote sensing images of 1999, 2008 and 2019 in the oasis area of the Taolai River Basin, a remote sensing image classification method based on ENVI deep learning was constructed to extract and identify the cover information of oasis area on the basis of establishing classification system, interpretation flags and sample data sets, and compared with the classification methods based on backpropagation neural network (BPNN), support vector machine regression (SVM) and random forest (RF). The results show that the overall accuracy of the classification method based on ENVI deep learning is 97.34 %, and the Kappa coefficient is 0.96; Under the same number of samples, compared with the classification method based on BPNN, SVM and RF, the classification method based on ENVI deep learning constructed in this study improves the overall accuracy by 6.80%, 2.04% and 3.03%, and the Kappa coefficient increases by 0.12, 0.07 and 0.09, respectively, and the classification method is the best for extracting surface cover information in oasis area. This study can provide technical support for rapid and accurate extraction and identification of ground cover information.

Keywords: remote sensing image, classification method, Kappa coefficient, deep learning, Oasis area

Introduction

As a critical interpretation technique, remote sensing image classification is widely used in the fields of earth monitoring, agriculture, and environmental science [1-3]. Remote sensing technology has advanced to the point where it can provide Earth observation data in a timely, multi-platform, and multi-temporal manner. Remote sensing image quality and quantity

have improved significantly [4]. The color texture information, ground object types, and spatial distribution of remote sensing images have become increasingly rich, diverse, and complex. However, remote sensing image classification is a complex data processing process. How a suitable classification method is selected or constructed is a critical factor in determining the success of remote sensing image classification.

Remote sensing image classification method research has always been a critical component of the field of remote sensing science. Numerous scholars have conducted extensive research on remote sensing

*e-mail: wenjuzhao@126.com

image classification in recent years and proposed many theories and models for remote sensing image classification [5-6]. Machine learning algorithms frequently use classification methods such as the artificial neural network (ANN) [7], the support vector machine (SVM) [8], and the random forest (RF) [9]. Li [10] enhanced the training process of a classical back-propagation neural network classifier. When compared to the classical algorithm, the proposed method significantly improved classification accuracy; Papp [11] used an ANN machine learning algorithm to classify vegetation in remote sensing images, and the ANN classification method performed better; Wang [12] proposed a remote sensing image classification method based on the optimal SVM, which is robust and adaptable; Al-Ali [13] noted that the support vector machine (SVM) machine learning algorithm is capable of extracting and identifying features effectively in arid environments. Izquierdo-Verdiguier [14] proposed an optimized RF classification method, with an overall classification accuracy improvement of nearly 6% over the baseline, indicating that the optimized RF has some potential for remote sensing image classification; Deur [15] demonstrated that the overall classification accuracy of the RF classification method based on WorldView-3 spectral features was 85%, that the classification accuracy could be increased by combining spectral and texture features, and that the overall classification accuracy could be increased by 10% compared to the gray level co-occurrence matrix classification method. Although these classification methods based on machine learning algorithms are capable of accurate classification, their level of automation is limited, and the feature information of ground objects cannot be fully utilized.

Deep learning has emerged as a new research direction in the field of machine learning as a result of the continuous advancement of artificial intelligence algorithms, providing novel ideas for the extraction and identification of remote sensing images [16-17]. Convolutional neural network (CNN), as one of the most representative algorithms of deep learning, has been widely used in remote sensing image classification research, and has accumulated many worthwhile results and experiences for remote sensing image classification research [18-21]. Pan [22] noted that CNNs can extract higher-level spatial features from images in a hierarchical manner, providing more powerful recognition capabilities for target detection and scene classification in high-resolution remote sensing images; Li [23] demonstrated that by using an improved CNN with an overlap pooling method for remote sensing image classification, image details can be effectively improved and obtain high classification accuracy. Although CNN has the advantages of high classification efficiency and classification accuracy in remote sensing image classification, it requires a large amount of training data, which often results in low classification efficiency and unstable classification accuracy due

to insufficient training data. The deep learning ENVI-Net is a fully convolutional neural network model architecture built based on the U-Net network architecture. Because of its features of fusing high and low-level semantic information, requiring less training data and fast training speed, the research of remote sensing image classification using the deep learning ENVI-Net is of great significance to enrich and improve the rapid and accurate extraction and identification of ground object information.

As an important area for human activities and industrial and agricultural development in the arid zone, the oasis area is the basis for the stable economic and social development of the region. Therefore, the use of remote sensing technology to rapidly and accurately classify and extract the land cover information of the oasis area is of great significance to the sustainable development and utilization of local water and soil resources. At present, deep learning has made great breakthroughs in the field of remote sensing image classification, and has achieved good results in the fields of large floating algae [24], mountain cultivated land [25] and alpine wetland classification [26]. However, there are few reports on the application of deep learning in the classification of land cover in arid oasis areas. The objectives of the study were to: (i) through field investigation, establish a suitable remote sensing image classification system, interpretation flags and sample data sets for arid oasis areas under the premise of ensuring applicability, scientific validity, and feasibility, (ii) construct a remote sensing image classification method based on ENVI deep learning, and extract and identify the surface cover information of oasis area by model training and model optimal parameters determination, (iii) comparative analysis classification methods based on backpropagation neural network (BPNN), support vector machine regression (SVM), random forest (RF) and classification methods based on ENVI deep learning, and determining the most suitable classification method for land cover information in the oasis area. This study provides technical support for the rapid and accurate extraction and recognition of land cover information.

Materials and Methods

Study Area

This paper selects a typical arid oasis area in the Taolai River basin as the study area. The study area is located in the central part of the Hexi Corridor in Gansu Province, between 97°22'46"-99°27'11"E and 38°24'16"-40°56'08"N (Fig. 1). The study area covers approximately 0.47 million km², and the terrain is generally elevated in the southwest and low in the northeast, sloping from southwest to northeast. The land cover types were classified and studied primarily by vegetation, construction land, water

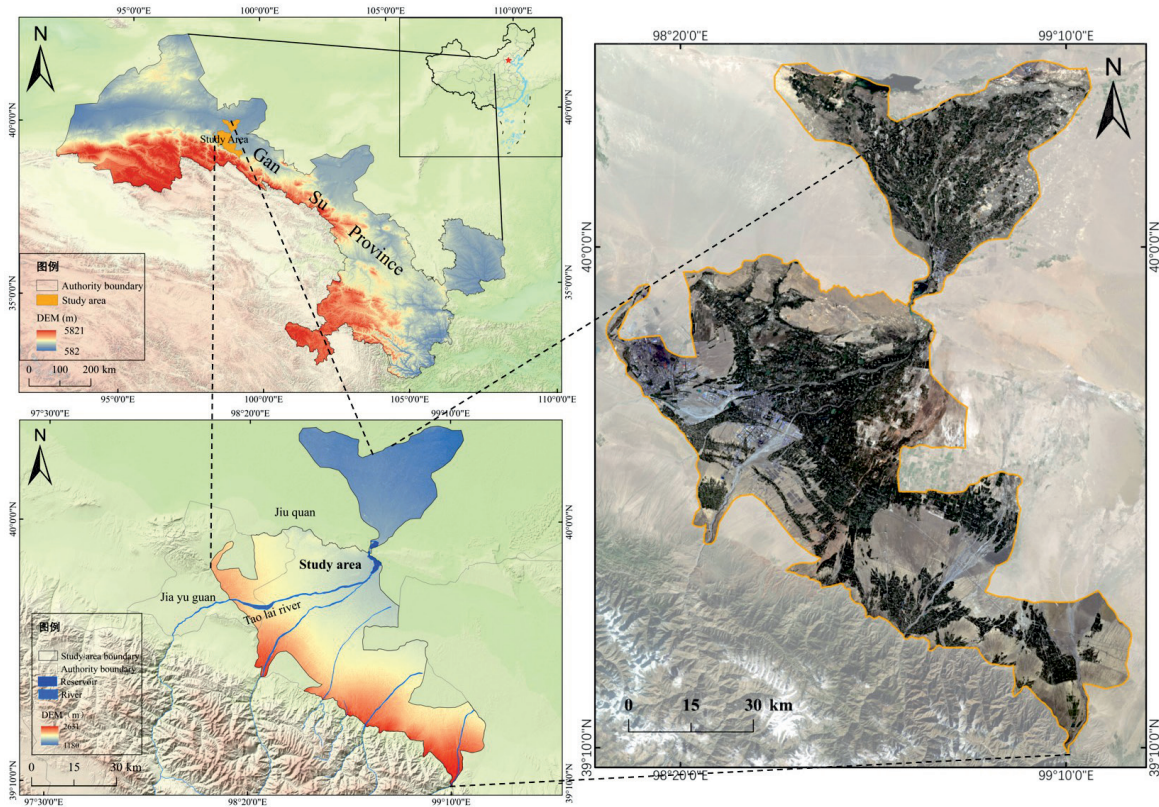


Fig. 1. The geographical location of the study area.

bodies, heavy saline land, medium saline land, light saline land, and bare land, in accordance with the study area's characteristics and the actual ground survey.

Research Methods

The technical process developed according to the experimental process is shown in Fig. 2. The specific experimental steps are: Firstly, the remote sensing image data preprocessing in the study area; Secondly, establish a suitable classification system, interpretation flags and sample data sets for the oasis area; Finally, a classification method based on ENVI deep learning is constructed to extract and identify the ground cover information of the oasis area, verify the generalization ability of the classification method, and compare it with the classification methods based on backpropagation neural network (BPNN), support vector machine regression (SVM), random forest (RF) to determine the most suitable classification method for the ground cover information of the oasis area.

Data Source and Preprocessing

The image data used in this paper were obtained from the official website of the United States Geological Survey (USGS) (<https://earthexplorer.usgs.gov/>) based on the geographical characteristics of the study area and the experimental requirements for obtaining remote sensing images. The images from July or August 1999,

2008, and 2019 were selected for three scenes every year because their cloudiness was less than 5%, and their image quality was higher, which was advantageous for the remote sensing image classification study (Table 1). To ensure the reliability of the experimental

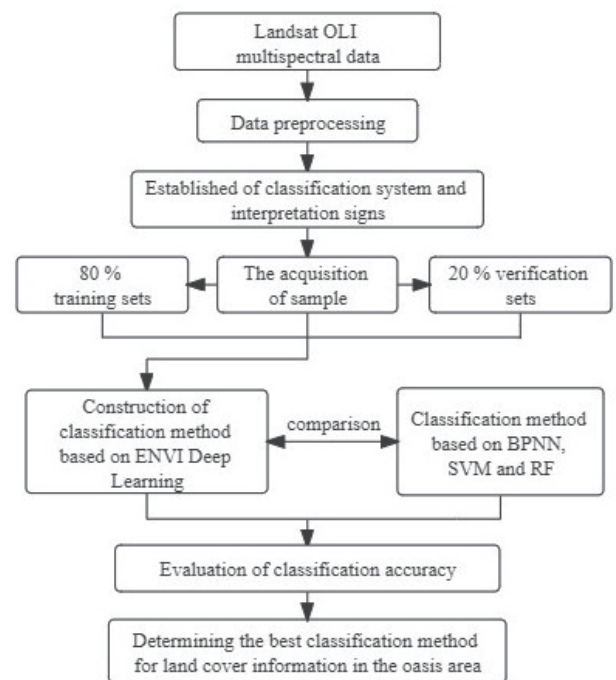


Fig. 2. The technique flow chart.

Table 1. The types of remote sensing data acquired in the study area.

Sensor Category	Year	Strip Number	Cloud Coverage	Imaging Time
Landsat TM	1999	Path 134~Row32	0.00%	1999/07/22
		Path 134~Row33	5.00%	1999/07/22
		Path 135~Row32	0.00%	1999/07/29
	2008	Path 134~Row32	0.00%	2008/08/31
		Path 134~Row33	1.00%	2008/08/31
		Path 135~Row32	0.00%	2008/08/22
Landsat OLI	2019	Path 134~Row32	0.00%	2019/07/29
		Path 134~Row33	1.15%	2019/07/29
		Path 135~Row32	2.62%	2019/08/05

results, image data from recent years were used, the spatial resolution of the acquired Landsat remote sensing images were 30 m, and Landsat remote sensing images were preprocessed with geometric correction, radiometric calibration, atmospheric correction, image mosaicking, and image cropping.

The field validation data in this article were collected via field surveys between May 20, 2021, and May 25, 2021. The collection of field verification data will directly affect the classification system and interpretation flags for remote sensing images. When collecting verification data, choose sample points with obvious ground object characteristics. Seven different types of field verification data were gathered: 75 Vegetation, 90 Construction Land, 65 Water Body, 60 Severe Salinized Land, and Moderate Salinized Land 65, Mild Salinized Land 80, Bare land 50, a total of 485.

A 4 km×4 km grid was established in the study area before the field survey, and the grid covered the whole study area. During the survey, GPS was used to obtain location information and record land-use types. Due to the inaccessibility of some lakes, kutang, sediments, and beaches for data collection, this paper used high-resolution Google Earth images to collect visual discrimination data for verification, and adjusted and gridded field survey data to compare the established classification sample system and the decoded signs for verification. Other auxiliary data included high-resolution Google Earth imagery and large-scale land-

use data in Gansu Province, which were used to assist in selecting training samples for training the model in the classification.

Establishment of the Classification System and Interpretation Flags

This paper used field surveys to record the actual feature types found in the study area (Fig. 3). The study area's remote sensing classification system was established using system standards from documents such as "Classification of Land Use Status GB/T21010-2017" (current), "Classification and Indicator System of Geographic State Information," and "Classification System of China Land Use Status Remote Sensing Monitoring Database" with the goal of ensuring applicability, scientificity, and feasibility. The classification system is divided into first- and second-level classification levels, with five first-level classification levels devoted to vegetation, construction land, water bodies, saline-alkali land, and bare land. Table 2 illustrates the classification system used to categorize remote sensing images in the study area.

The interpretation flags for remote sensing images of the study area were established based on the correspondence between remote sensing images and field survey conditions and on summarizing and analyzing the size, shape, shadow, texture, color, position, and other characteristics of various feature



Fig. 3. The types of field features in the study area.

Table 2. The remote sensing image classification system in the study area.

Serial Number	First Level Classification	Second Level Classification	Description
1	Vegetation		Including natural vegetation and artificial vegetation. Artificial vegetation is farmland, artificial green space, etc.; natural vegetation is primary and secondary vegetation, etc.
2	Construction Land		Including urban and rural residential areas, transportation and other land, factories, etc.
3	Water Body		Including rivers, lakes, reservoirs, ponds, etc.
4	Salinized Land	Severe Salinized Land	It refers to the land where the surface salinity collects heavily and no vegetation grows.
		Moderate Salinized Land	It refers to the land where salinity collects on the surface and only strong salinity-tolerant plants grow.
		Mild Salinized Land	It refers to land with slight or no saline aggregation on the surface, with little vegetation and only saline tolerant plants or saline tolerant crops.
5	Bare Land		Including bare land, Gobi, sand, bare rock, etc.

types on remote sensing images of the study area. The interpretation flags were created using remote sensing data from 1999, 2008, and 2019, as the sample data. The study area's remote sensing image interpretation flags are listed in Table 3.

Construction of Sample Dataset

1) Collection of training samples

When collecting samples, image samples with obvious features that are easy to interpret should be selected. The sample data sets are remote sensing image

data from 1999, 2008, and 2019, and the ROI Tool tool in ENVI software is used to define the sample name, sample color, and sample range, which completes the training sample acquisition. At the same time, the deviations in the training samples were adjusted and modified in accordance with the field validation data. Training samples were collected from 2936 vegetation samples, 1087 construction land samples, 1393 water body samples, 473 heavy saline samples, 313 medium saline samples, 347 light saline samples, and 371 bare land samples, totaling 6920 samples. Table 4 summarizes the results of the training sample collection.

Table 3. The remote sensing image interpretation flags in the study area.

Serial Number	Feature Type	Interpretation Flags	Logo Features
1	Vegetation		The color is dark red or light cyan mixed with red, mostly patchy, and the farmland vegetation has obvious regular border texture.
2	Construction Land		The color is more mixed, bluish-gray, with obvious borders and more irregular internal spots, or with obvious linear road features.
3	Water Body		The color is black or dark blue, the color texture is more uniform, and the shape is mostly irregular.
4	Severe Salinized Land		The color is mainly white or mixed with other light spots, with bright colors and irregular borders.
5	Moderate Salinized Land		The color is mainly magenta, mixed with white inside, with bright color and irregular texture of patches.
6	Mild Salinized Land		The color is mainly light orange or dark magenta, mixed with white or light green inside, with irregular texture of spots.
7	Bare Land		The color is mainly gray-green or dark gray-green, with obvious irregular texture.

Table 4. The statistical table of remote sensing image classification samples in the study area.

Sample Name	Number of Samples in 1999	Number of Samples in 2008	Number of Samples in 2019	Total
Vegetation	989	975	972	2936
Construction Land	363	358	366	1087
Water Body	462	470	461	1393
Severe Salinized Land	157	160	156	473
Moderate Salinized Land	106	102	105	313
Mild Salinized Land	113	122	112	347
Bare Land	127	128	1116	371
Total	2317	2315	2288	6920

2) Division of the sample data set

In this paper, Landsat satellite remote sensing image data in 1999 and 2008 are used as training set and verification set of classification method, and are divided into training set and verification set according to 80% and 20% of the total number of samples. The data in 2019 are used as test sets. The training set is used to train the model, and the validation set input the model with the training set but does not participate in the training, which is used to adjust the hyperparameters and evaluate the model. The test set is used to test the generalization ability of the model.

Classification Method and Evaluation Index

Classification Method Based on ENVI Deep Learning

The classification method based on ENVI deep learning comprises three distinct types of layers: convolutional, pooling, and deconvolutional, and the classification method based on ENVI deep learning completes the classification in the ENVI Deep Learning platform. The fundamental structural principle is as follows:

1) Convolutional layer: The convolution layer aims to extract various features via convolutional operations with various convolutional kernels. The formula for the convolution operation:

$$x_j^l = f\left(\sum_{i \in M_j} x_j^{l-1} * k_{ij}^l + b_j^l\right) \quad (1)$$

Where: x_j^l for the first-dimensional feature map of the l -th convolutional layer; $f()$ for the activation function; M_j for the set of $l-1$ layer feature maps; x_j^{l-1} for the i th feature map; k_{ij}^l for the i -th convolution kernel of the j -th dimensional feature map of the l -th layer convolution layer; b_j^l for the bias of the j -th dimensional feature map.

2) Pooling layer: The pooling layer is a downsampling layer, which serves to reduce the feature map, decrease the number of parameters, reduce the complexity and prevent overfitting. Pooling layer

calculation formula:

$$x_j^l = f(\beta_j^l \text{down}(x_j^{l-1}) + b_j^l) \quad (2)$$

Where: β_j^l for the weight of the j th dimensional feature map of the l th layer convolutional layer; $\text{down}()$ for the pooling function.

3) Deconvolutional layer: Deconvolution and anti-pooling are the inverse processes of convolution and pooling.

Other Classification Models

In this paper, classification methods based on backpropagation neural network (BPNN), support vector machine regression (SVM) and random forest (RF) are used to classify remote sensing images with the same number of samples. The purpose is to compare and verify the effectiveness and superiority of the proposed classification method based on ENVI deep learning.

Classification Model Accuracy Evaluation Index

Accuracy evaluation of remote sensing image classification is a critical component of remote sensing image classification technology, and accuracy analysis can be used to quantify the classification model's accuracy. The most frequently used method for evaluating the accuracy of remote sensing image classification is to analyze a confusion matrix. Four major evaluation indexes from the confusion matrix are chosen in this paper to assess the accuracy of classification results [27].

1) Overall accuracy: The overall accuracy (OA) measures the classification results' overall quality and is equal to the total number of pixels correctly classified divided by the total number of pixels. The following is the calculation formula:

$$OA = \sum_{i=1}^c m_{ii} / N \quad (3)$$

Where: c for the number of categories; m_{ii} for the elements on the diagonal of the confusion matrix; $N = \sum_{i=1}^c \sum_{j=1}^c m_{ij}$ for the total number of test samples.

2) Kappa coefficient: The Kappa coefficient is a multivariate discrete analysis technique used to quantify the degree of agreement between classification results and reference data. It considers all factors in the confusion matrix and serves as a more objective evaluation index; the larger the Kappa coefficient, the higher the classification accuracy. The following is the calculation formula:

$$k = N \cdot \frac{\sum_{i=1}^c m_{ii} - \sum_{i=1}^c m_{i+} m_{+i}}{N^2 - \sum_{i=1}^c m_{i+} m_{+i}} \quad (4)$$

Where: m_{i+} , m_{+i} for the sum of the i -th row and the sum of the i -th column of the confusion matrix, respectively.

3) User accuracy: The user accuracy (UA) value equals the ratio of pixels correctly classified into a particular class of features to the total number of pixels classified into that class. It is calculated by dividing the number of pixels on the diagonal of a particular class of features in the confusion matrix by the sum of the pixels in the same row as that class. The following is the calculation formula:

$$UA = X_{ij} / X_{*j} \quad (5)$$

Where: X_{ij} for the number of samples with land cover type j categorized as land cover type i ; X_{*j} for the number of samples whose total number of samples is classified as land cover type j .

4) Producer accuracy: The producer accuracy (PA) represents the ratio of the number of pixels correctly assigned to a class of features to the total number of real pixels of that class, and its value is equal to the number of pixels on the diagonal of a class of features in the matrix divided by the sum of the number of pixels in the same column as that class. The calculation formula is:

$$PA = X_{ij} / X_{i*} \quad (6)$$

Where: X_{ij} for the number of samples with land cover type j categorized as land cover type i ; X_{i*} for the number of samples whose total number of samples is classified as land cover type i .

Results and Discussion

Classification Results of Classification Methods Based on ENVI Deep Learning

Model Construction and Training Optimization

The process of building and training optimization of classification models based on ENVI deep learning in this paper is as follows: Firstly, the initialization model is created, the number of iterations of the attempted training is input in the Iterations of ENVI Deep Learning, and some parameters are preset according to prior knowledge. In the Randomize Parameters for Train TensorFlow Mask Model node, some training parameters are preset as fixed values, and other parameters are automatically randomly generated to better train the range of possible values of the best parameters. Secondly, after a certain number of iterative training, the TensorBoard visualization tool in ENVI deep learning is used to realize visual real-time tracking and evaluation of indicators such as the loss, accuracy, and precision during model training. Finally, on the basis of visual real-time tracking and evaluation, the optimal three sets of parameter settings are selected for re-evaluation. The sample data sets of 1999, 2008 and 2019 are used as training samples and verification samples. The random model training method in ENVI Deep Learning Guide Map is used to train the recognition method. Finally, a set of parameters with the most reliable classification effect are selected as the best parameters of the model, as shown in Table 5.

Post Processing

After classifying remote sensing images, the preliminary classification results will inevitably produce small spots, which will affect the production of classification maps. For this reason, this paper adopts the functions of Clump Classes, Sieve Classes and Majority Analysis post-processing in ENVI5.6 software to process the preliminary classification result map with small spots and correct any obvious errors, and finally make the remote sensing image classification map of the study area.

Classification Results of Classification Methods Based on ENVI Deep Learning

The study area's remote sensing images for the year 2019 were classified using the trained classification

Table 5. The best parameters for model training.

Parameter Name	Patch size	Number of Bands	Number of Epoches	Number of patches per Epoch	Number of patches per Batch	Patch Sampling Rate	Class Weight	Loss Weight
Parameter Value	572	3	25	500	5	16	2	2

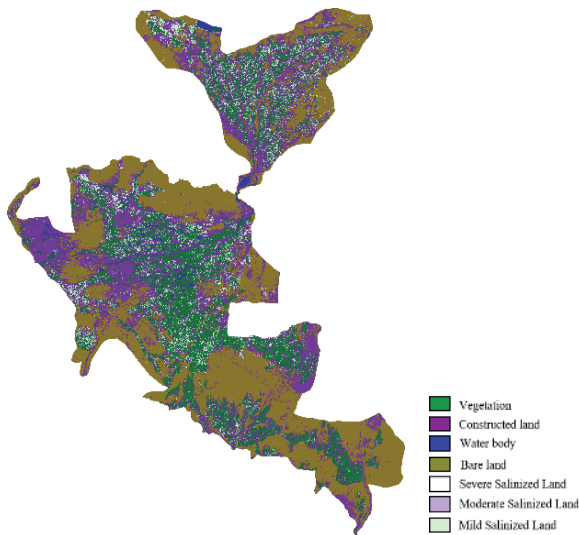


Fig. 4. The remote sensing image classification results of classification method based on ENVI deep learning.

method based on ENVI deep learning. Fig. 4 illustrates the classification results.

The classification results were evaluated using four evaluation indicators of overall accuracy, Kappa coefficient, user accuracy, and producer accuracy in the confusion matrix. The classification accuracy evaluation results are shown in Table 6.

As illustrated in Fig. 3, the classification method based on ENVI deep learning can significantly extract and identify different feature types for the year 2019. The classification results are more representative of the real surface distribution, with less misclassification and confusion between different feature types, which can more accurately reflect the study area’s real feature distribution characteristics.

As shown in Table 6, the classification method based on ENVI deep learning has better readability and maintains high classification accuracy in vegetation, water bodies, and bare land; there are fewer misclassifications between construction land and other types, especially in the calculation results of classification accuracy of saline land, the classification accuracy of heavy saline land is 97.93%, the classification accuracy of medium saline is 79.26%, and the classification accuracy of light saline is 84.68%; the overall classification accuracy of the classification method based on ENVI deep learning is 97.64%, and the kappa coefficient is 0.96. It demonstrates that the classification method based on ENVI deep learning possesses strong classification and generalization capabilities.

Comparative Evaluation with Other Classification Models

Under the same number of samples, the classification methods based on backpropagation neural network (BPNN), support vector machine regression (SVM), random forest (RF) and the classification method based on ENVI deep learning were compared the remote sensing images in the study area. Fig. 5 illustrates the Comparison of results of different classification methods.

As shown in Fig. 5 and Table 7, the classification method based on ENVI deep learning has the highest accuracy among the four classification methods under the same sample data, and the overall accuracy and Kappa coefficient are 97.64 % and 0.96. Compared with the classification methods based on backpropagation neural network (BPNN), support vector machine regression (SVM), random forest (RF), the classification method based on ENVI deep learning improves overall accuracy by 6.80%, 2.04%, and 3.08%, respectively,

Table 6. The classification accuracy evaluation results of classification method based on ENVI deep learning.

Year	Feature Type	Vegetation	Construction Land	Water Body	Bare Land	Severe Salinized Land	Moderate Salinized Land	Mild Salinized Land	User Accuracy (%)
2019	Vegetation	1450	1	0	0	0	0	9	99.32
	Construction Land	0	3046	16	585	9	0	1	83.29
	Water Body	0	3	7350	0	0	0	0	99.96
	Bare Land	0	34	7	17345	0	0	0	99.96
	Severe Salinized Land	0	0	0	0	189	3	1	97.93
	Moderate Salinized Land	0	0	0	0	2	107	26	79.26
	Mild Salinized Land	4	0	0	0	1	14	105	84.68
	Producer Accuracy (%)	1.00	0.99	1.00	0.97	0.94	0.86	0.74	
	Overall Accuracy (%)	97.64							
	Kappa Coefficient	0.96							

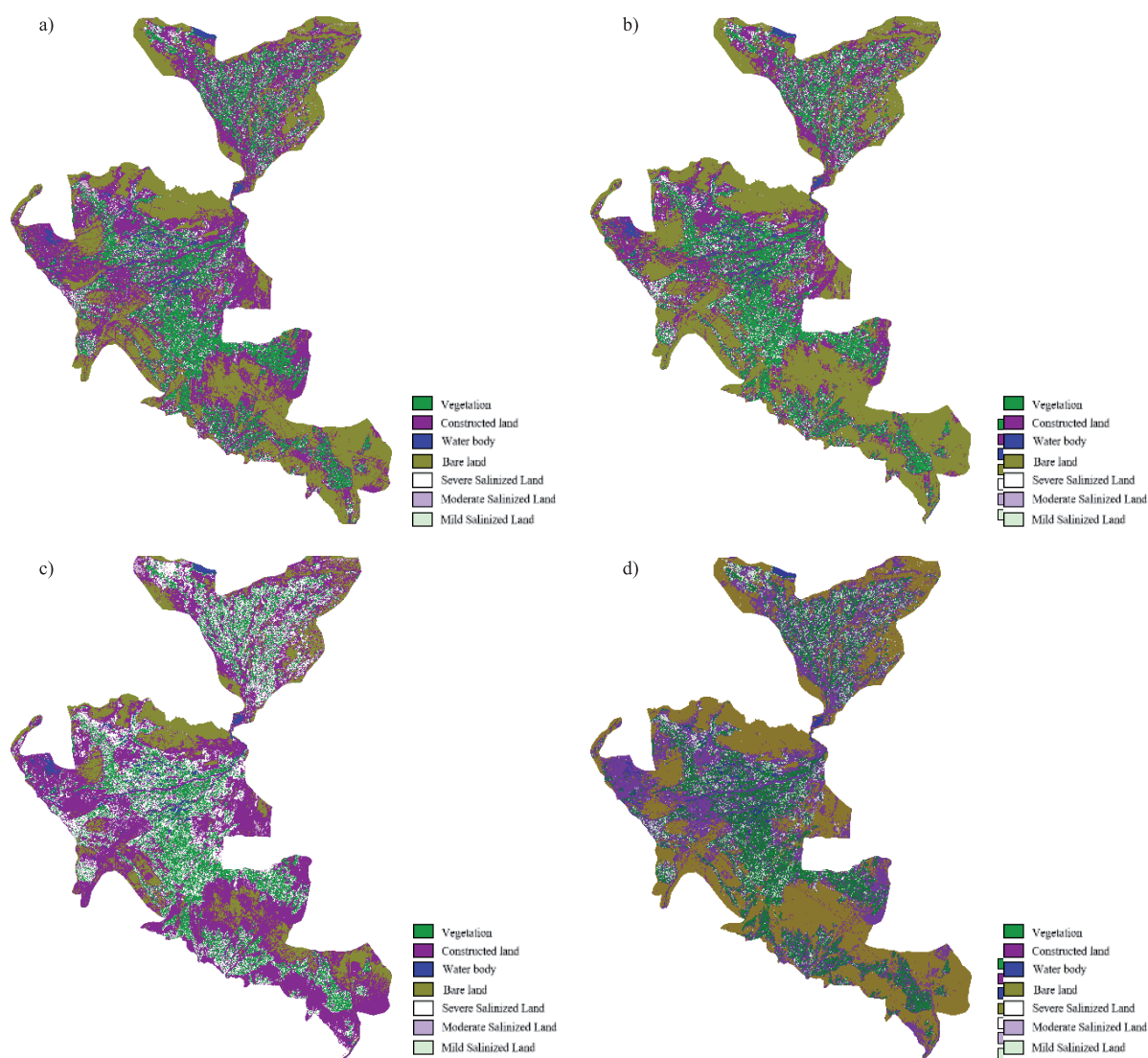


Fig. 5. The classification results of remote sensing images of the different classification methods.

and the Kappa coefficient by 0.12, 0.07, and 0.09. It demonstrates that the classification method based on ENVI deep learning can extract the distributing information of ground objects more effectively than the classification methods based on backpropagation neural network (BPNN), support vector machine regression (SVM), random forest (RF), and has good applicability, which can provide a theoretical basis for digital monitoring, reasonable development and sustainable development of water and soil resources in arid oasis areas, and has good applicability, which can provide some theoretical basis for the digital monitoring, rational development and sustainable development of soil and water resources in arid oasis areas.

Discussion

Remote sensing image classification is a critical interpretation technique because it enables the rapid extraction and identification of the rich semantic information contained in images. Accurately extracting and identifying information of different feature types are of great significance for digital monitoring and efficient and rational utilization of soil and water resources in the region. Convolutional neural networks (CNNs), the most representative deep learning algorithm, are widely used in research on remote sensing image classification [18-21]. Although CNN can adaptively extract the most relevant features to the classification

Table 7. The overall accuracy and Kappa coefficient of the different classification methods.

Classification Method	BPNN	SVM	RF	ENVI DL
Overall Accuracy (%)	90.84	95.60	94.61	97.64
Kappa Coefficient	0.84	0.89	0.87	0.96

target and performs better in remote sensing image classification, its shortcoming is that it requires massive data samples to improve classification accuracy [28-29]. After the continuous development and improvement of CNN, the development of classification methods such as fully convolutional neural network FCN, U-Net, DeepLab, etc. has compensated for the shortcomings such as CNN requires massive data samples for training and has the advantages of fusing high and low-level semantic information, requiring less training sample data, and fast training convergence [24-26, 30-32], which has also continuously enriched and improved the methods and theories of remote sensing image classification research and accumulated many worthy results and experiences [33-34].

In this study, the classification method based on ENVI deep learning was constructed using Landsat medium and low spatial resolution satellite remote sensing images and limited 6920 sample data, the overall classification accuracy of the classification method based on ENVI deep learning was 97.34%, and the Kappa coefficient is 0.96, indicating that the classification method has good classification ability with fewer training samples, it can extract and identify feature information better and has better classification ability. According to the user accuracy results, the classification method has a higher ability to identify vegetation, water bodies, and bare land using complex remote sensing image features at low and medium resolutions, but has a lower ability to discriminate linear features such as roads, which is primarily due to the low proportion of road samples in the training area. and is consistent with the findings of other researchers, such as [35-36], indicating that the classification method is still insufficient for acquiring image features and linear features. At the same time, when compared to the classification methods based on backpropagation neural network (BPNN), support vector machine regression (SVM), random forest (RF), the classification method based on ENVI deep learning improves overall classification accuracy by 8.09%, 1.60%, and 4.75%, respectively, the Kappa coefficient increased by 0.12, 0.05, and 0.09, respectively. Additionally, the study's results indicate that the classification method based on ENVI deep learning is reliable and outperforms machine learning algorithms on the same data sets in terms of classification, which is consistent with the findings of scholars such as [37-40]. The study provides technical support for the rapid and accurate extraction and recognition of land cover information.

The classification method based on ENVI deep learning developed in this paper has been used to perform classification studies on remote sensing images with low and medium spatial resolutions. It has produced satisfactory classification results. However, it is necessary to compare the classification results of remote sensing images with varying spatial resolutions to determine whether the classification method has a high degree of generalization for high spatial

resolution remote sensing images. As a result, additional research is required to determine the optimal spatial resolution for remote sensing data, optimize the deep learning algorithm, and fuse multi-source data.

Conclusions

In this paper, we conducted a remote sensing image classification study of the study area by developing a fully convolutional neural network ENVI-Net 5 classification model and comparing it to classification models developed using BPNN, SVM, and RF machine learning algorithms to verify the classification model's accuracy and reliability. The following are the major conclusions:

To establish two classification systems of primary and secondary classification of remote sensing images in arid oasis areas and corresponding interpretation flags through field investigation under the premise of ensuring applicability, scientific validity, and feasibility, and the remote sensing image data from 1999, 2008 and 2019 were used as the sample data sets, and collected totally 6920 samples, the 1999 and 2008 datas were used as the training and validation sets, and the 2019 datas were used as the test sets.

The constructed classification method based on ENVI deep learning can effectively extract and identify land cover information in arid oasis area on the basis of establishing a classification system, interpretation flags and sample data sets, the overall accuracy was 97.64%, and the Kappa coefficient was 0.96. It demonstrates that the classification method based on ENVI deep learning has good classification ability and generalization ability.

Among the four classification methods, the classification method based on ENVI deep learning was the most suitable classification method at present, compared with the classification methods based on backpropagation neural network (BPNN), support vector machine regression (SVM), random forest (RF), the classification method based on ENVI deep learning improves overall accuracy by 6.80%, 2.04%, and 3.03%, respectively, and the Kappa coefficient by 0.12, 0.07, and 0.09. It demonstrates that the classification method based on ENVI deep learning is reliable, and the study provides technical support for the rapid and accurate extraction and recognition of land cover information.

Acknowledgments

This study was supported by the National Natural Science Foundation of China (51869010).

Conflict of Interest

The authors declare no conflict of interest.

References

1. LYONS M.B., KEITH D.A., PHINN S.R., MASON T.J., ELITH J. A comparison of resampling methods for remote sensing classification and accuracy assessment. *Remote Sensing of Environment*. **208**, 145, **2018**.
2. ZAIDI S.M., AKBARI A., ABU SAMAH A., KONG N.S., GISEN A., ISABELLA J. Landsat-5 Time Series Analysis for Land Use/Land Cover Change Detection Using NDVI and Semi-Supervised Classification Techniques. *Polish Journal of Environmental Studies*. **26** (6), **2017**.
3. TAN K., ZHANG Y., WANG X., CHEN Y. Object-based change detection using multiple classifiers and multi-scale uncertainty analysis. *Remote Sensing*. **11** (3), 359, **2019**.
4. SAHA S., ZHAO S., ZHU X.X. Multitarget Domain Adaptation for Remote Sensing Classification Using Graph Neural Network. *IEEE Geoscience and Remote Sensing Letters*. **19**, 1, **2022**.
5. ORZECZOWSKA-SZAJDA I.D. Classification Model of Urban Riverside Landscape Using the Oder River as an Example. *Polish Journal of Environmental Studies*. **29** (1), **2020**.
6. XU C., ZHU G., SHU J. A lightweight intrinsic mean for remote sensing classification with lie group kernel function. *IEEE Geoscience and Remote Sensing Letters*. **18** (10), 1741, **2020**.
7. HARA P., PIEKUTOWSKA M., NIEDBALA G. Selection of independent variables for crop yield prediction using artificial neural network models with remote sensing data. *Land*. **10** (6), 609, **2021**.
8. SUN G., RONG X., ZHANG A., HUANG H., RONG J., ZHANG X. Multi-scale mahalanobis kernel-based support vector machine for classification of high-resolution remote sensing images. *Cognitive Computation*. **13** (4), 787, **2021**.
9. PENG K., JIANG W., DENG Y., LIU Y., WU Z., CHEN Z. Simulating wetland changes under different scenarios based on integrating the random forest and CLUE-S models: A case study of Wuhan Urban Agglomeration. *Ecological Indicators*. **117**, 106671, **2020**.
10. LI D., YANG F., WANG X. Study on ensemble crop information extraction of remote sensing images based on SVM and BPNN. *Journal of the Indian Society of Remote Sensing*. **45** (2), 229, **2017**.
11. PAPP L., VAN LEEUWEN B., SZILASSI P., TOBAK Z., SZATMARI J., ARVAI M., PASZTOR L. Monitoring invasive plant species using hyperspectral remote sensing data. *Land*. **10** (1), 29, **2021**.
12. WANG M., WAN Y., YE Z., LAI X. Remote sensing image classification based on the optimal support vector machine and modified binary coded ant colony optimization algorithm. *Information Sciences*. **402**, 50, **2017**.
13. AL-ALI Z.M., ABDULLAH M.M., ASADALLA N.B., GHOLOUM M. A comparative study of remote sensing classification methods for monitoring and assessing desert vegetation using a UAV-based multispectral sensor. *Environmental monitoring and assessment*. **192** (6), 1, **2020**.
14. IZQUIERDO-VERDIGUIER E., ZURITA-MILLA R. An evaluation of Guided Regularized Random Forest for classification and regression tasks in remote sensing. *International Journal of Applied Earth Observation and Geoinformation*. **88**, 102051, **2020**.
15. DEUR M., GASPAROVIC M., BALENOVIC I. Tree species classification in mixed deciduous forests using very high spatial resolution satellite imagery and machine learning methods. *Remote Sensing*. **12** (23), 3926, **2020**.
16. SHELHAMER E., LONG J., DARRELL T. Fully convolutional networks for semantic segmentation. *IEEE transactions on pattern analysis and machine intelligence*. **39** (4), 640, **2016**.
17. SHARMA A., LIU X., YANG X., SHI D. A patch-based convolutional neural network for remote sensing image classification. *Neural Networks*. **95**, 19, **2017**.
18. WANG J., SHEN L., QIAO W., DAI Y., LI Z. Deep feature fusion with integration of residual connection and attention model for classification of VHR remote sensing images. *Remote Sensing*. **11** (13), 1617, **2019**.
19. LI Y., LIU C., ZHAO W., HUANG Y. Multi-spectral remote sensing images feature coverage classification based on improved convolutional neural network. *Mathematical Biosciences and Engineering*. **17** (5), 4443, **2020**.
20. PALLY R.J., SAMADI S. Application of image processing and convolutional neural networks for flood image classification and semantic segmentation. *Environmental Modelling & Software*. **148**, 105285, **2022**.
21. KUMAR D.A. Knowledge-Based Morphological Deep Transparent Neural Networks for Remote Sensing Image Classification. *IEEE Journal of Selected Topics in Applied Earth Observations and Remote Sensing*. **15**, 2209, **2022**.
22. PAN X., ZHAO J., XU J. An object-based and heterogeneous segment filter convolutional neural network for high-resolution remote sensing image classification. *International Journal of Remote Sensing*. **40** (15), 5892, **2019**.
23. LI C., YANG S.X., YANG Y., GAO H., ZHAO J., QU X., GAO J. Hyperspectral remote sensing image classification based on maximum overlap pooling convolutional neural network. *Sensors*. **18** (10), 3587, **2018**.
24. WANG M., HU C. Satellite remote sensing of pelagic Sargassum macroalgae: The power of high resolution and deep learning. *Remote Sensing of Environment*. **264**, 112631, **2021**.
25. YU L., HU Z., ZHANGG F., YANG K. Unmanned aerial vehicle image biological soil crust recognition based on UNet++. *International Journal of Remote Sensing*. **43** (7), 2660, **2022**.
26. ZHANG B., ZHAO L., ZHANG X. Three-dimensional convolutional neural network model for tree species classification using airborne hyperspectral images. *Remote Sensing of Environment*. **247**, 111938, **2020**.
27. YE F., AI T., WANG J., YAO Y., ZHOU Z. A Method for Classifying Complex Features in Urban Areas Using Video Satellite Remote Sensing Data. *Remote Sensing*. **14** (10), 2324, **2022**.
28. DING X., LI Y., YANG J., LI H., LIU L., LIU Y., ZHANG C. An adaptive capsule network for hyperspectral remote sensing classification. *Remote Sensing*. **13** (13), 2445, **2021**.
29. PAN X., ZHAO J., XU J. An object-based and heterogeneous segment filter convolutional neural network for high-resolution remote sensing image classification. *International Journal of Remote Sensing*. **40** (15), 5892, **2019**.
30. SHRESTHA S., VANNESCHI L. Improved fully convolutional network with conditional random fields for building extraction. *Remote Sensing*. **10** (7), 1135, **2018**.
31. MOHAMMADIMANESH F., SALEHI B., MAHDIANPARI M., GILL E., MOLINIER M. A new fully convolutional neural network for semantic segmentation of polarimetric SAR imagery in complex

- land cover ecosystem. *ISPRS journal of photogrammetry and remote sensing*. **151**, 223, **2019**.
32. SHAO Z., TANG P., WANG Z., SALEEM N., YAM S., SOMMAI C. BRRNet: A fully convolutional neural network for automatic building extraction from high-resolution remote sensing images. *Remote Sensing*. **12** (6), 1050, **2020**.
 33. CAO K., ZHANG X. An improved res-unet model for tree species classification using airborne high-resolution images. *Remote Sensing*. **12** (7), 1128, **2020**.
 34. SUN Y., LIU B., YU X., YU A., XUE Z., GAO K. Resolution reconstruction classification: fully octave convolution network with pyramid attention mechanism for hyperspectral image classification. *International Journal of Remote Sensing*. **43** (6), 2076, **2022**.
 35. LIN Y., XU D., WANG N., SHI Z., CHEN Q. Road extraction from very-high-resolution remote sensing images via a nested SE-DeepLab model. *Remote sensing*. **12** (18), 2985, **2020**.
 36. WANG Y., GAO L., HONG D., SHA J., LIU L., ZHANG B., ZHANG Y. Mask DeepLab: End-to-end image segmentation for change detection in high-resolution remote sensing images. *International Journal of Applied Earth Observation and Geoinformation*. **104**, 102582, **2021**.
 37. PENG M., ZHANG L., SUN X., CEN Y., ZHAO X. A Synchronous Long Time-Series Completion Method Using 3-D Fully Convolutional Neural Networks. *IEEE Geoscience and Remote Sensing Letters*. **19**, 1, **2021**.
 38. YE Z., FU Y., GAN M., DENG J., COMBER A., WANG K. Building extraction from very high resolution aerial imagery using joint attention deep neural network. *Remote Sensing*. **11** (24), 2970, **2019**.
 39. SI Y., GONG D., GUO Y., ZHU X., HUANG Q., EVANS J., SUN Y. An Advanced Spectral – Spatial Classification Framework for Hyperspectral Imagery Based on DeepLab v3+. *Applied Sciences*. **11** (12), 5703, **2021**.
 40. NIU Z., LIU W., ZHAO J., JIANG G. DeepLab-based spatial feature extraction for hyperspectral image classification. *IEEE Geoscience and Remote Sensing Letters*. **16** (2), 251, **2018**.